Measurement 151 (2020) 107160

Contents lists available at ScienceDirect

Measurement

journal homepage: www.elsevier.com/locate/measurement

Curvature detection in a medical needle using a Fabry-Perot cavity as an intensity sensor

Susana Novais [a,*], Susana O. Silva [a], Orlando Frazão [a,b]

[a] INESC TEC – Institute for Systems and Computer Engineering, Technology and Science, Rua do Campo Alegre 687, 4169-007 Porto, Portugal
[b] Department of Physics and Astronomy, Faculty of Sciences of University of Porto, Rua do Campo Alegre 687, 4169-007 Porto, Portugal

ARTICLE INFO

Article history:
Received 17 June 2019
Received in revised form 7 October 2019
Accepted 13 October 2019
Available online 18 October 2019

Keywords:
Needle interventions
Fabry-Perot cavity
Curvature measurement
Tip position
Optical fiber sensor

ABSTRACT

The use of optical sensors inside the needle can improve targeting precision and can bring real-time information about the location of the needle tip if necessary, since a needle bends through insertion into the tissue. Therefore, the precise location of the needle tip is so important in percutaneous treatments. In the current experiment, a fiber sensor based on a Fabry-Perot (FP) cavity is described to measure the needle curvature. The sensor is fabricated by producing an air bubble between two sections of multimode fiber. The needle with the sensor therein was attached at one end and deformed by the application of movements. The sensor presents a sensitivity of −0.152 dB/m^{-1} to the curvature measurements, with a resolution of 0.089 m^{-1}. The sensory structure revealed to be stable, obtaining a cross-sensitivity to be 0.03 m^{-1}/°C.

1. Introduction

Medical applications require minimally invasive sensors, particularly for in-vivo procedure. For instance, it is very common in surgical medical interventions or even for medical diagnosis the use of needles for insertion in soft tissues. Therefore, it is extremely important developing miniaturized sensors that are capable of being incorporated into such needles and be capable of measuring physical, chemical, or biochemical parameters [1,2].

The Fabry-Perot (FP) interferometers can be a type of sensing structure to be explored due to the ability of producing sensing probes that can be optically interrogated in a reflection configuration [3]. Due to the small dimensions and its optical characteristics the FP interferometers have great potential, they can be effortlessly incorporated in innovative structures and are one of the most utilized interferometers [4,5]. It can be employed for detecting an extensive range of physical parameters, such as, displacement [6,7], lateral load [8], temperature [9,10], vibration [11,12], refractive index [10,13] and curvature [5,14,15]. Compared to the other electrical sensors, the optical fiber sensors afford an important solution for curvature measurements due to their intrinsic characteristics, such as compact dimensions, lightweight, capability of multiplexing, immunity to electromagnetic interference, chemical inertness, and the ability to resist corrosion [16].

Taking into account the concept of modulation, the optical fiber curvature sensor can be sectioned into different classifications, namely: frequency modulation [16,17], wavelength modulation [18] and intensity modulation [19,20]. The first work based on the fiber micro-bend sensor, was proposed in 1980, by Fields and Cole [21]. In last years, several optical fiber curvature sensors, have been developed, including photonic crystal fiber [14,15], fiber Bragg gratings [22,23], long period fiber gratings [24,25], multicore fiber [26,27], fiber tapers and fiber lateral-offset splicing [28,29] and Fabry-Perot [15,30].

From the literature it is known that different optical fiber curvature sensors have previously been used for medical purposes. For instance, to monitoring the radius of curvature of rotary endodontic file within an artificial channel [31], and for monitoring the needle curvature/deflection [1,31–34].

To diagnose certain diseases in patients it is necessary to collect tissue samples and for this procedure the use of needles is recurrent, therefore it is crucial monitored the accuracy of the needle upon reaching a target tissue, in order to avoid errors in the detection of target tissue, which could lead to misdiagnoses and repeated insertions and consequently hemorrhages [35]. For all these reasons, it is extremely important to monitoring the curvature of the needle to avoid problems when it is introduced toward into a soft tissue.

In this study, an intensity fiber sensor based on a Fabry-Perot cavity made by splicing two sections of multimode fiber is demonstrated. The sensing structure was incorporated into a

* Corresponding author.
E-mail address: susana.novais@inesctec.pt (S. Novais).

https://doi.org/10.1016/j.measurement.2019.107160
0263-2241/

medical needle and characterized for curvature measurements. To our cognizance, it is the first time that the curvature of a medical needle with a Fabry-Perot sensor has been studied.

2. Sensing structure and operation mode

The sensors produced in this work were developed by producing an air cavity between two sections of graded-index multimode fiber (MMF GIF625). The MMF GIF625, have an Ø62.5 μm core/Ø125 μm cladding and can be used as a sensor element [36,37].

The technique used to manufacture the sensing structures is adapted from a previous works presented by the author [8]. Fig. 1 presents a layout of the FP sensor exploited, an image taken from the microscope of the cavity produced, having a diameter of 225 μm, and a photograph with the insertion of the optical fiber inside the needle. This sensor structure is manufactured by joining a multimode fiber fused to a single-mode fiber.

The operation mode of the sensor relies on excitation of higher-order modes along the graded-index multimode fiber section that will illuminate the Fabry-Perot cavity.

The back-reflected light traveling through the MMF depends on the geometry of the microsphere. Then, a part of this light will be guided back by the SMF, since the acceptance angle acts as a filter [38].

2.1. Experimental setup and calibration

Fig. 2 displays the layout of the experimental setup used in this work, for the curvature experiments, in a classic reflection scheme. The experimental setup consisted on a broadband optical source centered at 1550 nm, with a bandwidth of 100 nm, an optical spectrum analyzer (OSA Yokogama, AQ6370C) with a resolution of 0.01 dB and the sensing structure coupled by means an optical circulator.

The needle used throughout this work has a 70 mm long and has an internal diameter of 0.34 mm, whereas the uncoated optical fiber diameter is 0.125 mm. The FP sensor has been introduced into the needle and positioned about 10 mm from the tip of the needle.

The axis shown in Fig. 2 indicates the direction of needle displacement in the curvature measurements performed. The y^+ and y^- corresponds to the nomenclature right and left presented in Figs. 3–5.

2.2. Experimental results and discussion

In curvature study the handle of the needle was fixed on the adjustable platform and piled up on the topside of the ruler and one displacement along the needle was applied with a one-dimensional translation stage. The curvature formulation can be tailored according to Eq. (1) [39]:

$$C = \frac{1}{R} = \frac{2d}{d^2 + L^2} \quad (1)$$

where *C, R, L* and *d* are curvature, bending radius, distance between the adjustable platform, and the displacement distance of the platform, respectively.

Fig. 3 presents the spectral behavior of the FP cavity without curvature. Analyzing the reflection spectrum arranged in the center of that Fig. 3, this one can be appraised to a two-wave interferometer. The free spectral range (FSR), can be calculated by the subtraction of the wavelengths of adjoining peaks, $\Delta\lambda = \lambda_2 - \lambda_1$, and this FSR is influenced by two parameters, —i.e. by the size of the cavity, L_{FP}, that can be calculated across the Eq. $\Delta\lambda = \lambda_1\lambda_2/(2n_{eff}L_{FP})$, and by the effective refractive index (n_{eff} (λ)). Taking into account that the manufactured air bubble cavity is only constituted by air, and by measuring the length of cavity thru the two adjacent peaks wavelengths extracted from the spectral response, and by the microscope images, it was determined that the cavity had a size of 225 μm and it was still estimated that the n_{eff}, within the cavity was ~1.00.

A curvature study was carried out using a translation stage and subjecting the needle with the sensor to curvature variations. The needle was placed parallel to the translation stage and a displacement was applied (recall Fig. 2). In the inset of Fig. 3 are shown the reflection spectra of the developed cavity, during the curvature tests in the needle for one positive (right) and negative (left) displacement, respectively. As it is possible to observe by Fig. 3, in both cases there is a variation in light intensity. This is due to the variation of the curvature radius which will influence the coupling efficiency of the FP mirrors.

The optical power response of the both rotations on the needle is shown on Fig. 4. Taking into account the reproducibility of the sensor structure, the experiments were all performed 3 times, (inset of Fig. 4) considering different displacements of curvature and after analyzing the average of the results was presented (Fig. 4). Based on the results achieved, it is considered that there is good repeatability, evidencing the robustness and reversibility of the sensor. During all cycles a minimum of the correlation factor of 0.976 and 0.990 were obtained for the left and right curvature displacements, respectively.

As shown in Fig. 4, it is clear the relationship between the sensing structure and the rotation of the needle. By turning the needle 90°, the sensing structure only has a residual sensitivity to curvature, since it is located in the neutral line, while with a 0° rotation

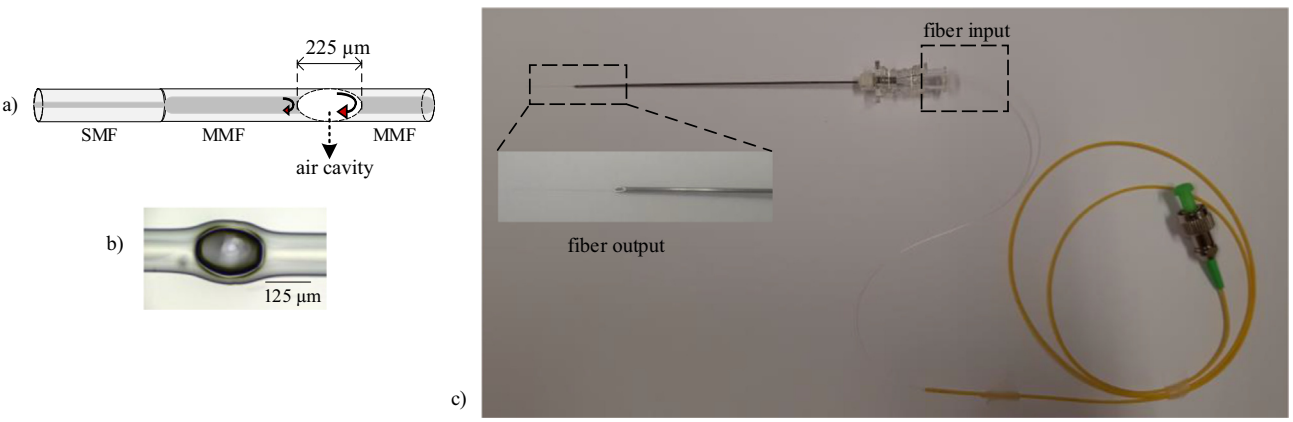

Fig. 1. a) Scheme, b) microscope photograph of the FP cavity and c) photograph of the FP inserted into the needle.

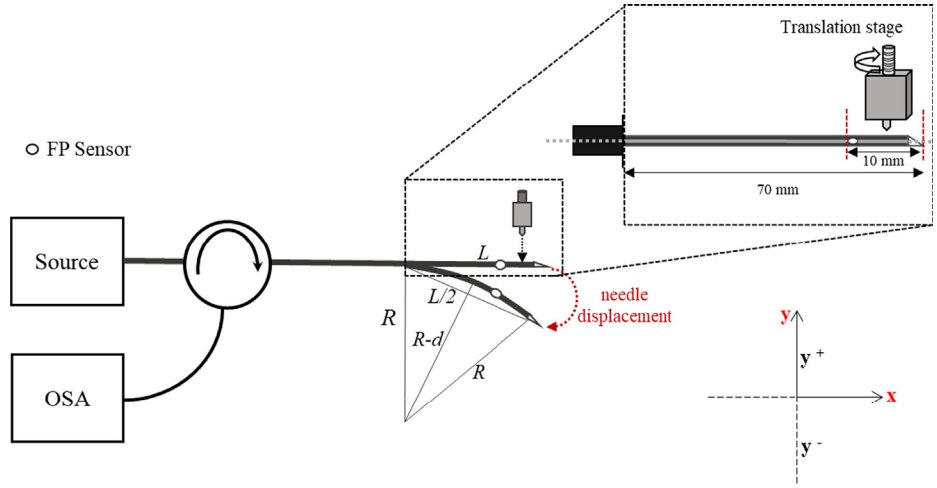

Fig. 2. Layout of the experimental setup highlighting top view of needle with FP cavity location, where *R*, *L* and *d*, are bending radius, distance between the adjustable platform and the displacement distance of the platform, respectively.

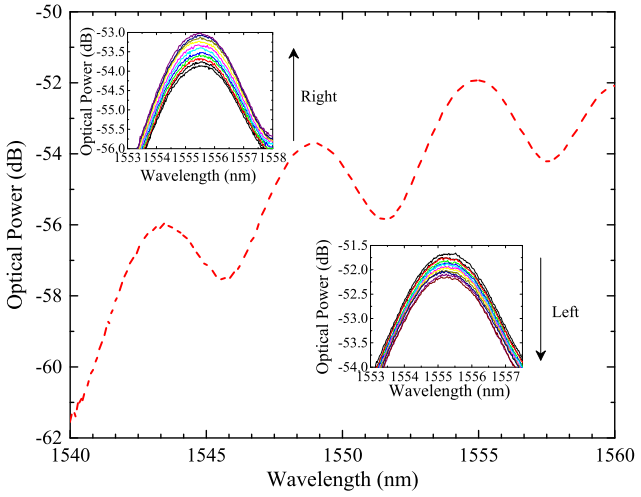

Fig. 3. Reflection spectrum of FP cavity without curvature applied (inset: optical reflective spectra for different displacements on the needle).

of the needle, a maximum sensitivity of -0.152 ± 0.006 dB/m^{-1} is achieved.

Depending on the therapeutic medical intervention, the curvature of the needle is adapted, therefore monitoring this parameter is extremely important. For instance, if a surgical procedure where a straight insertion in soft tissue is necessary, the use of rigid needles is crucial, thus, is so important to be able to monitor small changes in curvature. However, if it is necessary to reach targets that may be camouflaged by other tissues, it is necessary to use very flexible needles, with high curvature, —i.e. with small radius of curvature.

Fig. 5 presents the relation between the optical and the radius of curvature. This result shows that the sensor is suitable for radius of curvature between ~−845 mm and ~820 mm, ideal for different medical applications [40,41].

The sensor stability was also explored. The sensor was exposed to diverse curvature measurements, during 90 min at room temperature, and the curvature response was attained each minute.

The optical variations with time, is shown in Fig. 6 and the mean value was of -53.009 ± 0.001 dB. The minimum value of curvature, δ_C that the sensor is able to discriminate, is given by Eq. (2), [42]:

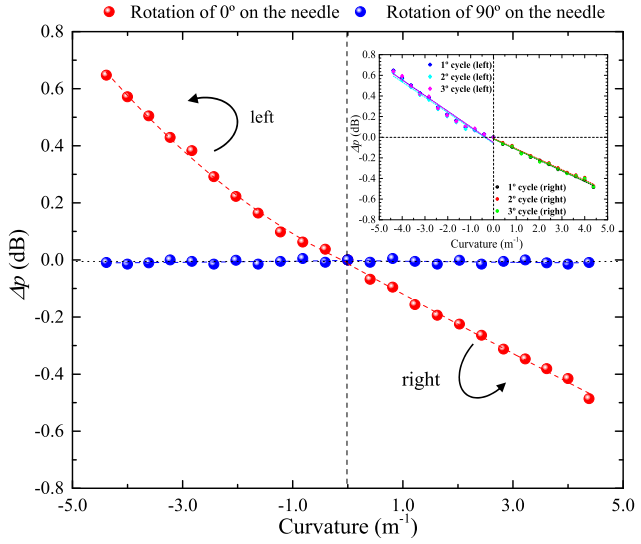

Fig. 4. Curvature responses of the FP cavity for different rotations.

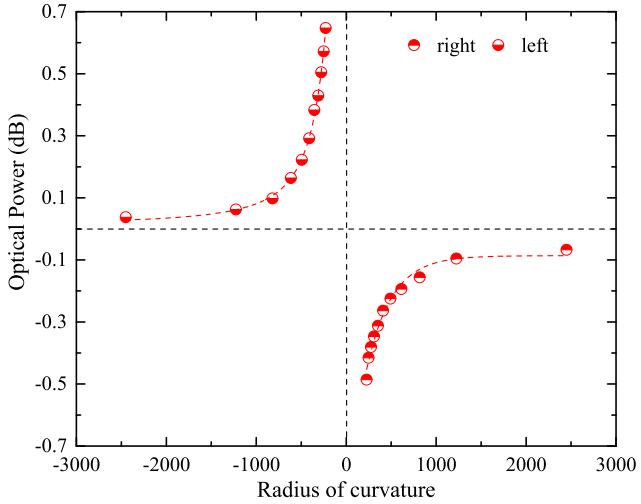

Fig. 5. Radius of curvature responses of the FP cavity.

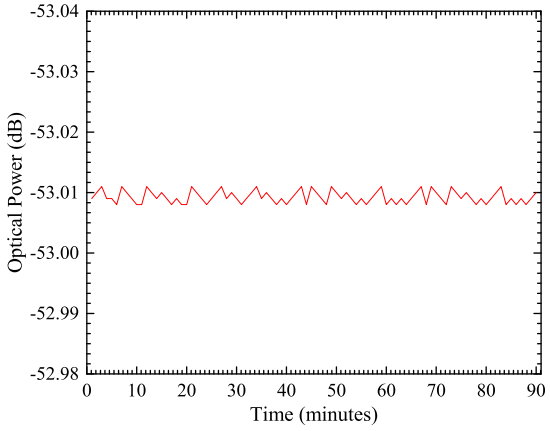

Fig. 6. Long term stability experiment.

$$\delta_C = 2\frac{\sigma_P \Delta C}{\Delta P} \quad (2)$$

where σ_P is the standard deviation of optical power for both values of curvature, and ΔC and ΔP are the variation of curvature and the mean of optical power between the two steps, respectively. By applying Eq. (2), a resolution of 0.089 m^{-1} was obtained. It is important to note that this value is also influenced by the spectral resolution of the equipment used for data acquisition (0.01 dB).

The temperature response of the FP cavity was also studied. The FP was positioned in a thermal chamber (Model 340, challenge Angelantoni Industry) , where temperature varied from 10 °C to 100 °C, maintained ca. 30 min at each step ensure temperature stabilization, and the optical power variations were controlled using the same interrogation scheme as shown in Fig. 2. The same process for the cooling was followed, and the proposed sensor exhibited very low thermal dependence ($4.87 \times 10^{-3} \pm 0.002$ dB/°C). A cross-sensitivity of 0.03 m^{-1}/°C was acquired between the temperature and curvature.

According to the Circadian rhythms, the body temperature of a healthy individual oscillates throughout the day, reaching a variation from the beginning of the morning towards the end of the afternoon, ca. 0.5 °C [43,44]. Assuming the sensitivity obtained at temperature and curvature, it can be concluded that a body thermal variation of 0.5 °C corresponds to a variation of -0.015 m^{-1} in curvature, this value still being within the range of error of the cross-sensitivity obtained, and can thus be negligible.

3. Final remarks

A curvature sensor based on a Fabry-Perot cavity was demonstrated. The sensing structure was fabricated by using the electric arc discharge method to create an air bubble between two sections of multimode fibers. The sensor structure was subjected to tests of curvature and temperature, obtaining a maximum sensitivity of -0.152 ± 0.006 dB/m^{-1}. Furthermore, the FP cavity demonstrated insignificant sensitivity to temperature, demonstrating a maximum cross-sensitivity of 0.03 m^{-1}/°C. The projected sensor shown strong stability, the results are repeatable and the manufacturing technique of the sensing structure, can arise as a substitute to other techniques, by the ease of reproducibility, the reduced cost of the manufacturing process and by the fact that no chemical solutions are involved to do chemical etching in the fibers.

Such measures can be considered an additional value both medicine and industry. In the hospital environmental can help in different surgical procedures that require precision when inserting the needles into different soft tissues and also assist health professionals to more effectively manage the handling of the needle to avoid sensitive tissue that might be located along the path to the target. For industry, this sensor can be used as a complementary test in bending control in the manufacture of medical needles.

Ethical Approval

Work on human beings that is submitted to *Medical Engineering & Physics* should comply with the principles laid down in the Declaration of Helsinki; Recommendations guiding physicians in biomedical research involving human subjects. Adopted by the 18th World Medical Assembly, Helsinki, Finland, June 1964, amended by the 29th World Medical Assembly, Tokyo, Japan, October 1975, the 35th World Medical Assembly, Venice, Italy, October 1983, and the 41st World Medical Assembly, Hong Kong, September 1989. You should include information as to whether the work has been approved by the appropriate ethical committees related to the institution(s) in which it was performed and that subjects gave informed consent to the work.

Declaration of Competing Interest

The authors declare that they have no known competing financial interests or personal relationships that could have appeared to influence the work reported in this paper.

Acknowledgments

This work is financed by the ERDF – European Regional Development Fund through the Operational Programme for Competitiveness and Internationalization – COMPETE 2020 Programme and by National Funds through the Portuguese funding agency, FCT (Portugal) – *Fundação para a Ciência e a Tecnologia* within project ENDOR – Endoscope based on New Optical Fibre Technology for Raman Spectroscopy (POCI-01-0145-FEDER-029724).

References

[1] A. Monen, M. Kemp, S. Misra, 3D flexible needle steering in soft-tissue phantoms using fiber bragg grating sensors, in: International Conference on Robotics and Automation, Proc. IEEE, 2013, pp. 5823–5829, https://doi.org/10.1109/ICRA.2013.6631418.

[2] N. Abolhassani, R.V. Patel, M. Moallem, Needle insertion into soft tissue: a survey, Med. Eng. Phys. 29 (8) (2007) 413–431, https://doi.org/10.1016/j.medengphy.2006.07.003.

[3] A.D. Gomes, M. Becker, J. Dellith, M.I. Zibaii, H. Latifi, M. Rothhard, et al., Multimode fabry-perot interferometer probe based on vernier effect for enhanced temperature sensing, Sensors 453 (18) (2018) 1–9, https://doi.org/10.3390/s19030453.

[4] Z. Tao, D. Wu, M. Liu, D.W. Duan, In-line fiber optic interferometric sensors in single-mode fibers, Sensors 12 (8) (2012) 10430–10449, https://doi.org/10.3390/s120810430.

[5] D. Jauregui-Vazquez, J.M. Estudillo-Ayala, A. Castillo-Guzman, R. Roja-Laguna, R. Selvas-Aguilhar, E. Vargas-Rodriguez, et al., Highly sensitive curvature and displacement sensing setup based on all fiber micro Fabry-Perot interferometer, Opt. Commun. 308 (1) (2013) 289–292, https://doi.org/10.1016/j.optcom.2013.07.041.

[6] N. Lagakos, T. Litovitz, P. Macedo, R. Mohr, R. Meister, Multimode optical fiber displacement sensor, Appl. Opt. 20 (2) (1981) 167, https://doi.org/10.1364/AO.20.000167.

[7] L.A. Ferreira, A.B. Lobo Ribeiro, J.L. Santos, F. Farahi, Simultaneous measurement of displacement and temperature using a low finesse cavity and a fiber Bragg grating, Photonics Technol. Lett. 8 (11) (1996) 1519–1521, https://doi.org/10.1109/68.541569.

[8] S. Novais, M.S. Ferreira, J.L. Pinto, Lateral load sensing with an optical fiber inline microcavity, Photonics Technology Letters. 29 (17) (2017) 1502–1505, https://doi.org/10.1109/LPT.2017.2735021.

[9] Q. Rong, H. Sun, X. Qiao, J. Zhang, M. Hu, Z. Feng, A miniature fiber-optic temperature sensor based on a Fabry-Perot interferometer, J. Opt. 14 (4) (2012), https://doi.org/10.1088/2040-8978/14/4/045002.

[10] M. Jiang, E. Gerhard, A simple strain sensor using a thin film as a low-finess fiber-optic Fabry-Perot interferometer, Sensors Actuators A: Phys. 88 (1) (2011) 41–46, https://doi.org/10.1016/S0924-4247(00)00494-5.

[11] B. Dong, J. Hao, T. Zhang, J.L. Lim, High sensitive fiber-optic liquid refractive index tip sensor based on a simple inline hollow glass micro-sphere, Sens. Actuators, B 171 (2012) 405–408, https://doi.org/10.1016/j.snb.2012.05.001.
[12] Q. Zhang, T. Zhu, Y. Hou, K.S. Chiang, All-fiber vibration sensor based on a Fabry-Perot interferometer and a microstructure beam, J. Opt. Soc. Am. B. 30 (5) (2013) 1211–1215, https://doi.org/10.1364/JOSAB.30.001211.
[13] S. Novais, Ferreira Ms, J.L. Pinto, Optical fiber Fabry Perot tip sensor for detection of water-glycerin mixtures, J. Lightwave Technol. 36 (9) (2018) 1576–1582, https://doi.org/10.1109/JLT.2017.2784540.
[14] H. Gong, H. Song, X. Li, J. Wang, X. Dong, An optical fiber curvature sensor based on photonic crystal fiber modal interferometer, Sens. Actuators, A 195 (6) (2013) 139–141, https://doi.org/10.1016/j.sna.2013.02.022.
[15] S.M. Catarina, M.S. Ferreira, S.O. Silva, J. Kobelke, K. Shuster, J. Bierlich, O. Frazão, Fiber fabry-perot interferometer for curvature sensing, Photonics Sensors. 6 (4) (2016) 339–344, https://doi.org/10.1007/s13320-016-0333-9.
[16] D. Zheng, J. Madrigal, D. Barrera, S. Sales, J. Copmany, Microwave photonic filtering for interrogating FBG-based multicore fiber curvature sensor, IEEE Photonics Technol. Lett. 29 (20) (2017) 1707–1710, https://doi.org/10.1109/LPT.2017.2742579.
[17] Y. Zhao, M.-Q. Chen, F. Xia, R.-Q. Lv, Small In-fiber Fabry-Perot low-frequency acoustic pressure sensor with PDMS diaphragm embedded in hollow-core fiber, Sens. Actuators, A 270 (2018) 162–169, https://doi.org/10.1016/j.sna.2017.12.057.
[18] C.M. Sterke, N.G.R. Broderik, Coupled-mode equations for periodic superstructure Bragg gratings, Opt. Lett. 20 (20) (1995) 2039–2041, https://doi.org/10.1364/OL.20.002039.
[19] T.G. Giallorenzi, J.A. Bucaro, A. Dandrige, G.H. Sigel, J.H. Cole, S.C. Rashleigh, R. G. Priest, Optical fiber sensor technology, IEEE Trans. Microw. Theory Tech. 30 (4) (1982) 472–511, https://doi.org/10.1109/TMTT.1982.1131089.
[20] V. Bhatia, K.A. Murphy, R.O. Claus, T.A. Tran, J.A. Greene, Recent developments in optical-fiber-based extrinsic Fabry-Perot interferometric strain sensing technology, Smart Mater. Struct. 4 (4) (1995) 246–251, https://doi.org/10.1088/0964-1726/4/4/004.
[21] J.N. Fields, J.H. Cole, Fiber micro bend acoustic sensor, Appl. Opt. 19 (19) (1980), https://doi.org/10.1364/AO.19.3265_1.
[22] H.J. Patrick, G.M. Williams, A.D. Kersey, J.R. Pedrazzani, A.M. Vengsarkar, Hybrid fiber Bragg grating/long period fiber grating sensor for strain/temperature discrimination, IEEE Photonics Technol. Lett. 8 (9) (1996) 1223–1225, https://doi.org/10.1109/68.531843.
[23] Y.X. Jin, C.C. Chan, X.Y. Dong, F.Y. Zhang, Bending sensor with tilted fiber bragg grating interacting with multimode fiber, Opt. Commun. 282 (19) (2009) 3905–3907, https://doi.org/10.1016/j.optcom.2009.06.058.
[24] O. Frazão, J. Viegas, P. Caldas, J.L. Santos, F.M. Araújo, L.A. Ferreira, F. Farahi, All-fiber Mach-Zehnder curvature sensor based on multimode interference combined with a long-period grating, Opt. Lett. 32 (21) (2007) 3074–3076, https://doi.org/10.1364/OL.32.003074.
[25] L.-Y. Shao, A. Laronche, M. Smietana, P. Mikulic, W.J. Bock, J. Albert, Highly sensitive bend sensor with hybrid long-period and tilted fiber Bragg grating, Opt. Commun. 283 (13) (2016) 2690–2694, https://doi.org/10.1016/j.optcom.2010.03.013.
[26] I. Floris, S. Sales, P.A. Calderón, J.M. Adam, Measurement uncertainty of multicore optical fiber sensors used to sense curvature and bending direction, Measurement 132 (2019) 35–46, https://doi.org/10.1016/j.measurement.2018.09.033.
[27] I. Floris, P.A. Calderón, S. Sales, J.M. Adam, Effects of core position uncertainty on optical shape sensor accuracy, Measurement 139 (2019) 21–33, https://doi.org/10.1016/j.measurement.2019.03.031.
[28] P. Lu, L. Men, K. Sooley, Q. Chen, Tapered fiber Mach-Zehnder interferometer for simultaneous measurement of refractive index and temperature, Appl. Phys. Lett. 94 (2009) 131110–131111, https://doi.org/10.1063/1.3115029.
[29] X. Wen, T. Ning, H. You, J. Li, T. Feng, L. Pei, W. Jian, Dumbbell-shaped Mach–Zehnder interferometer with high sensitivity of refractive index, IEEE Photon. Technol. Lett. 25 (18) (2013) 1839–1842, https://doi.org/10.1109/LPT.2013.2277611.
[30] M. Cano-Contreras, A.D. Guzman-Chavez, R.I. Mata-Chavez, E. Vargas-Rodriguez, D. Jauregui-Vazquez, D. Claudio-Gonzalez, et al., All-fiber curvature sensor based on an abrupt tapered fiber and a Fabry-Pérot interferometer, IEEE Photonics Technol. Lett. 26 (22) (2014) 2213–2216, https://doi.org/10.1109/LPT.2014.2349979.
[31] C.-S. Shin, M.-W. Lin, An optical fiber-based curvature sensor for endodontic files inside a tooth root canal, IEEE Sens. J. 10 (6) (2010) 1061–1065, https://doi.org/10.1109/JSEN.2010.2040077.
[32] R.J. Roesthuis, M. Kemp, J.J. Dobbelsteen, S. Misra, Three-dimensional needle shape reconstruction using an array of fiber bragg grating sensors, IEEE/ASME Trans. Mechatronics. 19 (4) (2014) 1115–1126, https://doi.org/10.1109/TMECH.2013.2269836.
[33] Y.-L. Park, S. Elayaperumal, B. Daniel, S.C. Rye, M. Shin, J. Savall, R.J. Black, et al., MRI-compatible haptics: Feasibility of using optical fiber Bragg grating strain-sensors to detect deflection of needles in an MRI environment, International Society for Magnetic Resonance in Medicine (ISMRM), 16th Scientific Meeting and Exhibition, 2008.
[34] K. Henken, D.V. Gerwen, J. Dankelman, J.J. Dobbelsteen, Accuracy of needle position measurements using fiber Bragg grating, Minimally Invasive Therapy 21 (2012) 408–414, https://doi.org/10.3109/13645706.2012.666251.
[35] M. Kaya, E. Senel, A. Ahmad, O. Bebek, Visual needle tip tracking in 2D US guided robotic interventions, Mechatronics 57 (2019) 129–139, https://doi.org/10.1016/j.mechatronics.2018.12.002.
[36] Y. Gong, Yu Guo, Y.-J. Rao, T. Zhao, Y. Wu, Curvature and temperature discrimination using multimode interference fiber optic structures – A proof of concept, IEEE Photonics Technol. Lett. 23 (23) (2010) 1708–1710, https://doi.org/10.1109/LPT.2010.2082518.
[37] D. Donlagic, B. Culshaw, Propagation of the fundamental mode in curved graded index multimode fiber and its application in sensor systems, J. Lightwave Technol. 18 (83) (2000) 334–340, https://doi.org/10.1109/50.827505.
[38] D. Donlagic, M. Zavrsnik, Fiber-optic microbend sensor structure, Opt. Lett. 22 (11) (1997) 837–839, https://doi.org/10.1364/OL.22.000837.
[39] G. Fu, Y. Li, Q. Li, J. Yang, X. Fu, W. Bi, Temperature insensitive vector bending sensor based on asymmetrical cascading SMF-PCF-SMF structure, IEEE Photonics J. 9 (3) (2017) 7103114, https://doi.org/10.1109/JPHOT.2017.2692277.
[40] M. Khadem, C. Rossa, N. Usmani, R.S. Sloboda, M. Tavakoli, Introducing notched flexible needles with increased deflection curvature in soft tissue 16340787, in: IEEE International Conference on Advanced Intelligent Mechatronics (AIM), 2016, https://doi.org/10.1109/AIM.2016.7576931.
[41] K.A. Troy, J.D. Greer, P.F. Laeseke, G.L. Hwang, A.M. Okumura, Methods for Improving the Curvature of Steerable Needles in Biological Tissue, IEEE Transactions on Biomedical Engineeing. 63 (6) (2016) 1167–1177, https://doi.org/10.1109/TBME.2015.2484262.
[42] S. Novais, M.S. Ferreira, J.L. Pinto, Relative humidity fiber sensor based on multimode interferometer coated with agarose-gel, Coatings. 8 (453) (2018), https://doi.org/10.3390/coatings8120453].
[43] P.A. Mackowiak, M.D. Mackowiak, S.S. Wasserman, Levine MM.A critical appraisal of 98.6 degrees F, the upper limit of the normal body temperature, and other legacies of Carl Reinhold August Wunderlich, J. Am. Med. Assoc. 268 (12) (1992) 1578–1580, https://doi.org/10.1001/jama.1992.03490120092034.
[44] S.-L. Märtha, R.N. Forberg, L.K. Wahren, Normal oral, rectal, tympanic and axillary body temperature in adult men and women: a systematic literature review, Scand. J. Caring Sci. 16 (2) (2002) 122–128, https://doi.org/10.1046/j.1471-6712.2002.00069.x.